

# A local discontinuous Galerkin method for the compressible Reynolds lubrication equation

Iñigo Arregui, J. Jesús Cendán and María González

*Dpto. de Matemáticas, Universidade da Coruña, Campus de Elviña s/n, 15071 A Coruña (Spain) and CITIC, Campus de Elviña, 15071 A Coruña (Spain)*

---

## Abstract

We present an extension of the local discontinuous Galerkin (LDG) method introduced in [9] for nonlinear diffusion problems to nonlinear stationary convection-diffusion problems. We develop a numerical study of the convergence properties of the new method and solve the stationary compressible Reynolds lubrication equation under some realistic conditions.

*Keywords:* Reynolds equation, discontinuous Galerkin method, hydrodynamic problem, convection-diffusion

---

## 1. Introduction

Discontinuous Galerkin (DG) methods were introduced in 1973 by Reed and Hill [25] for solving the neutron transport equation. These methods have been successfully applied to the solution of convection-diffusion equations when convection is dominant [16, 18, 15, 22, 23, 17, 14, 27]. Indeed, Cockburn and Shu [16] introduced the so-called Local Discontinuous Galerkin (LDG) method as an extension to general convection-diffusion problems of the numerical scheme proposed by Bassi and Rebay [5] for the compressible Navier-Stokes equations.

In general, these methods have the disadvantage of requiring more degrees of freedom than usual continuous Galerkin methods. However, their high degree of accuracy can compensate this drawback. In [18] a multiscale discontinuous Galerkin (MDG) method that has the computational structure and cost of a conforming method was introduced, and later analyzed in [7, 20]. On the other hand, a hybridizable discontinuous Galerkin method for convection-diffusion-reaction problems was proposed in [15]. This method shows optimal convergence properties for both the total flux and the scalar variable. Moreover, it exhibits superconvergence properties for the approximation of the scalar variable. In [22], a different approximation for the total flux is considered and the method is extended to time-dependent linear convection-diffusion equations. Steady-state and time-dependent nonlinear convection-diffusion equations with smooth solution are considered in [23].

More recently, the discontinuous Galerkin method was combined with a mixed method to solve a linear stationary convection-diffusion problem [17], a method based on the interior penalty discontinuous Galerkin (IPDG) method was proposed in [14] for the same equation, and the nonsymmetric DG method with interior penalties (NIPG) and the symmetric DG method with interior penalties (SIPG) on modified graded meshes were analyzed in [27].

We are interested in the numerical solution of the compressible Reynolds lubrication equation modified for slip flow. This equation arises, for instance, in the modelling of read/write processes in magnetic storage devices, such as hard disks [6]. It is a nonlinear convection-dominated convection-diffusion equation. Concerning its one-dimensional version, in [19] a Locally exact Partial Differential Equation Method (LPDEM), combined with a Newton-Raphson method was applied. On the other hand, an algorithm based on the approximation by characteristics of the convection dominating terms and a duality method to treat the nonlinear diffusive term was studied in one [2] and two dimensions [3] (see also [11]). However, up to the authors' knowledge, regardless their possible advantages, no discontinuous Galerkin methods have been applied to solve this equation.

In this work we explore the applicability of a local discontinuous Galerkin method introduced in [9] for nonlinear diffusion problems to nonlinear stationary convection-diffusion equations. We develop a numerical study of the convergence properties of the method and solve the two-dimensional compressible Reynolds lubrication equation modified for slip flow in several academic and realistic situations.

The paper is organized as follows. Section 2 briefly describes the compressible Reynolds lubrication equation modelling the hydrodynamic behaviour of magnetic reading devices. In Section 3, we present the extension of the method introduced in [9] to a general nonlinear stationary convection-diffusion equation. In Section 4 we describe the flux formulation. Then, in Section 5 we provide some numerical results for the compressible Reynolds lubrication equation modified for slip flow. Finally, in Section 6 we draw some conclusions.

## 2. The compressible Reynolds lubrication equation

The compressible Reynolds lubrication equation models thin gas films. For example, in magnetic recording devices (such as computer hard disks) an air layer flows between the rigid disk, where the data are stored, and the reading head. In this case, as both bodies are rigid, the thickness (or gap) of the air layer is a known function. In other kinds of devices, the data are stored in a flexible magnetic tape; thus, the air gap is not known a priori and has to be computed, jointly with the air pressure, as the solution of a coupled elasto-hydrodynamic problem [26].

In an isothermal and stationary regime, compressible Reynolds equation for

a (perfect) gas lubricating film with pure sliding conditions is [6]:

$$\nabla \cdot \left[ \frac{ph^3}{\eta} \nabla p \right] = 6 \frac{\partial}{\partial x_1} (Uph),$$

where  $x_1$  and  $x_2$  are the spatial coordinates ( $x_1$  is the coordinate in the direction of sliding),  $\eta$  is the viscosity of the gas,  $U$  is the sliding velocity of the moving bearing surface (which we will assume to be constant),  $h$  is the local film thickness and  $p$  is the local pressure of the gas.

Following Burgdorfer [8], local viscosity  $\eta$  is related to viscosity at ambient conditions,  $\eta_a$ , by:

$$\eta = \frac{\eta_a}{1 + 6a\lambda/h},$$

where  $a$  and  $\lambda$  are parameters related to the surface and the gas, respectively. Introducing the Knudsen number at ambient conditions,  $M$ , the viscosity can be written as:

$$\eta = \frac{\eta_a}{1 + 6aMp_a h_m / (ph)},$$

where  $p_a$  is the ambient pressure and  $h_m$  is the mean film thickness. Thus, Reynolds equation becomes:

$$\nabla \cdot \left[ ph^3 \left( 1 + \frac{6aMp_a h_m}{ph} \right) \nabla p \right] = 6\eta_a \frac{\partial}{\partial x_1} (Uph). \quad (1)$$

As it is usual in other fluid mechanics models, we introduce adimensional variables:

$$P = \frac{p}{p_a}, \quad H = \frac{h}{h_m}, \quad X_1 = \frac{x_1}{L}, \quad X_2 = \frac{x_2}{L},$$

where  $L$  is a characteristic dimension of the domain. Then (1) takes the following form:

$$\nabla \cdot \left[ \left( 1 + \frac{6aM}{PH} \right) PH^3 \nabla P \right] = \frac{6\eta_a UL}{p_a h_m^2} \frac{\partial}{\partial X_1} (PH). \quad (2)$$

Introducing the bearing number

$$\Lambda = \frac{6\eta_a UL}{p_a h_m^2}$$

leads us to:

$$\Lambda \frac{\partial}{\partial X_1} (PH) - \nabla \cdot \left[ \left( 1 + \frac{6aM}{PH} \right) PH^3 \nabla P \right] = 0$$

or, in an equivalent form,

$$\frac{\partial}{\partial X_1} (PH) - \nabla \cdot [\alpha H^2 \nabla P + \beta H^3 P \nabla P] = 0, \quad (3)$$

where the constant coefficients are given by:

$$\alpha = \frac{6aM}{\Lambda} \quad \text{and} \quad \beta = \frac{1}{\Lambda}.$$

Thus, for usual values of parameters [6] we have

$$\alpha = 3.32 \times 10^{-3}, \quad \beta = 7.01 \times 10^{-4}$$

so that the linear contribution to diffusion is sensibly larger than the nonlinear one.

### 3. A local discontinuous Galerkin method for nonlinear stationary convection-diffusion equations

Let  $d = 2, 3$  and let  $\Omega \subset \mathbb{R}^d$  be a polygonal or polyhedral domain with boundary  $\Gamma$ . We consider the following nonlinear convection-diffusion problem: find  $u : \Omega \rightarrow \mathbb{R}$  such that

$$\begin{cases} \sum_{i=1}^d \partial_{x_i} \left( f_i(u) - \sum_{j=1}^d a_{ij}(u) \partial_{x_j} u \right) = l & \text{in } \Omega \\ u = g & \text{on } \Gamma \end{cases} \quad (4)$$

where  $f_i, a_{ij}, l$  and  $g$  are sufficiently smooth given functions.

We follow [9] and introduce as auxiliary unknowns the gradient,  $\mathbf{s} = \nabla u$ , and the total flux,  $\boldsymbol{\sigma}$ , with components  $\sigma_i = \sum_{j=1}^d a_{ij}(u) s_j$ , for  $i = 1, \dots, d$ , in  $\Omega$ . Then, problem (4) can be rewritten equivalently as follows:

$$\begin{cases} \mathbf{s} = \nabla u & \text{in } \Omega, \\ \sigma_i = \sum_{j=1}^d a_{ij}(u) s_j, \quad \text{for } i = 1, \dots, d & \text{in } \Omega, \\ \sum_{i=1}^d \partial_{x_i} f_i(u) - \nabla \cdot \boldsymbol{\sigma} = l & \text{in } \Omega, \\ u = g & \text{on } \Gamma. \end{cases} \quad (5)$$

Let  $\{\mathcal{T}_h\}_h$  be a regular family of triangulations of  $\Omega$ , made up of triangles if  $d = 2$  or tetrahedra if  $d = 3$ , where  $\Omega = \cup_{T \in \mathcal{T}_h} T$ . We multiply the first three equations of problem (5) by smooth test functions  $\boldsymbol{\tau}, \mathbf{t}$  and  $v$ , respectively, and integrate over an element  $T \in \mathcal{T}_h$ :

$$\begin{cases} \int_T \mathbf{s} \cdot \boldsymbol{\tau} = \int_T \nabla u \cdot \boldsymbol{\tau}, \\ \int_T \boldsymbol{\sigma} \cdot \mathbf{t} = \int_T \sum_{i=1}^d \sum_{j=1}^d a_{ij}(u) s_j t_i, \\ \int_T \sum_{i=1}^d \partial_{x_i} f_i(u) v - \int_T \nabla \cdot \boldsymbol{\sigma} v = \int_T l v, \end{cases}$$

where  $u = g$  on  $\Gamma$ .

Integrating by parts in the first and third equations, we have

$$\left\{ \begin{array}{l} \int_T \mathbf{s} \cdot \boldsymbol{\tau} + \int_T u \nabla \cdot \boldsymbol{\tau} - \int_{\partial T} u \boldsymbol{\tau} \cdot \mathbf{n}_T = 0, \\ \int_T \sum_{i=1}^d \sum_{j=1}^d a_{ij}(u) s_j t_i - \int_T \boldsymbol{\sigma} \cdot \mathbf{t} = 0, \\ \int_T \sum_{i=1}^d \partial_{x_i} f_i(u) v + \int_T \boldsymbol{\sigma} \cdot \nabla v - \int_{\partial T} \boldsymbol{\sigma} \cdot \mathbf{n}_T v = \int_T l v, \end{array} \right. \quad (6)$$

where  $\mathbf{n}_T$  is the unit outward normal to  $T$ . Moreover,  $u = g$  on  $\Gamma$ .

Let  $k$  be a nonnegative integer. We denote by  $\mathcal{P}_k(T)$  the space of polynomials of degree at most  $k$  on  $T$ . Then, we consider the discrete spaces

$$V_h^k := \{v_h \in L^2(\Omega) : v_h|_T \in \mathcal{P}_k(T), \quad \forall T \in \mathcal{T}_h\}$$

and

$$\Sigma_h^k := \{\boldsymbol{\tau}_h \in [L^2(\Omega)]^d : \boldsymbol{\tau}_h|_T \in [\mathcal{P}_k(T)]^d, \quad \forall T \in \mathcal{T}_h\}.$$

We then approximate the exact solution  $(\mathbf{s}, u, \boldsymbol{\sigma})$  by  $(\mathbf{s}_h, u_h, \boldsymbol{\sigma}_h) \in \Sigma_h^{k_1} \times V_h^{k_2} \times \Sigma_h^{k_3}$  (in general, we will take  $k_1 = k_2 = k_3$  or  $k_1 = k_3 = k_2 - 1$ ).

The idea of the local discontinuous Galerkin method is to enforce the conservation laws given in (6) by substituting the values of  $\boldsymbol{\sigma}$  and  $u$  on  $\partial T$  by appropriate numerical approximations  $\hat{\boldsymbol{\sigma}}$  and  $\hat{u}$ , respectively. We consider the following formulation: find  $(\mathbf{s}_h, u_h, \boldsymbol{\sigma}_h) \in \Sigma_h^{k_1} \times V_h^{k_2} \times \Sigma_h^{k_3}$  such that for all  $T \in \mathcal{T}_h$ ,

$$\left\{ \begin{array}{l} \int_T \mathbf{s}_h \cdot \boldsymbol{\tau}_h + \int_T u_h \nabla \cdot \boldsymbol{\tau}_h - \int_{\partial T} \hat{u} \boldsymbol{\tau}_h \cdot \mathbf{n}_T = 0, \\ \int_T \sum_{i=1}^d \sum_{j=1}^d a_{ij}(u_h) (\mathbf{s}_h)_j (\mathbf{t}_h)_i - \int_T \boldsymbol{\sigma}_h \cdot \mathbf{t}_h = 0, \\ \int_T \sum_{i=1}^d \partial_{x_i} f_i(u_h) v_h + \int_T \boldsymbol{\sigma}_h \cdot \nabla v_h - \int_{\partial T} \hat{\boldsymbol{\sigma}} \cdot \mathbf{n}_T v_h = \int_T l v_h, \end{array} \right.$$

for all  $(\mathbf{t}_h, v_h, \boldsymbol{\tau}_h) \in \Sigma_h^{k_1} \times V_h^{k_2} \times \Sigma_h^{k_3}$ , where the numerical fluxes  $\hat{\boldsymbol{\sigma}}$  and  $\hat{u}$  usually depend on  $\boldsymbol{\sigma}_h, u_h$  and the boundary conditions; in particular,  $\hat{u} = g$  on  $\Gamma$ .

In order to define the specific numerical fluxes that we will employ in our formulation, we need to introduce some notations. Let  $T$  and  $T'$  be two adjacent elements in  $\mathcal{T}_h$ . Then, an *interior edge (face)* of  $\mathcal{T}_h$  is the (nonempty) interior of  $\partial T \cap \partial T'$ ; analogously, if  $T$  is a boundary element of  $\mathcal{T}_h$ , a *boundary edge (face)* of  $\mathcal{T}_h$  is the (nonempty) interior of  $\partial T \cap \Gamma$ . We denote by  $\mathcal{E}_I$  the union of all interior edges (faces) of  $\mathcal{T}_h$ , by  $\mathcal{E}_\partial$  the union of all boundary edges (faces), and by  $\mathcal{E} := \mathcal{E}_I \cup \mathcal{E}_\partial$ .

Given  $v := (v_T)_{T \in \mathcal{T}_h} \in \Pi_{T \in \mathcal{T}_h} L^2(\partial T)$  and  $\boldsymbol{\tau} := (\boldsymbol{\tau}_T)_{T \in \mathcal{T}_h} \in \Pi_{T \in \mathcal{T}_h} [L^2(\partial T)]^d$ , we denote by  $v_{T,e} := v_T|_e$  and  $\boldsymbol{\tau}_{T,e} := \boldsymbol{\tau}_T|_e$ ,  $\forall T \in \mathcal{T}_h$  and  $\forall e \in \mathcal{E}$ . Let  $e \in \mathcal{E}_I$ ,

$e = \partial T \cap \partial T'$ . Then, we define the *average* of  $v$  on  $e$  as

$$\{v\} := \frac{1}{2}(v_{T,e} + v_{T',e})$$

and the *jump* of  $v$  across  $e$  as

$$[v] := v_{T,e} \mathbf{n}_T + v_{T',e} \mathbf{n}_{T'}.$$

Analogously, we define the *average* and the *jump* of  $\boldsymbol{\tau}$  across  $e \in \mathcal{E}_I$  as

$$\{\boldsymbol{\tau}\} := \frac{1}{2}(\boldsymbol{\tau}_{T,e} + \boldsymbol{\tau}_{T',e}), \quad [\boldsymbol{\tau}] := \boldsymbol{\tau}_{T,e} \cdot \mathbf{n}_T + \boldsymbol{\tau}_{T',e} \cdot \mathbf{n}_{T'}.$$

We remark that  $[v]$  is a vector whereas  $[\boldsymbol{\tau}]$  is a scalar quantity.

Let  $e \in \mathcal{E}_\partial$ . Since the traces of  $v$  and  $\boldsymbol{\tau}$  are defined in a unique way, we denote

$$[v] := v_{T,e} \mathbf{n}_T, \quad \{\boldsymbol{\tau}\} := \boldsymbol{\tau}_{T,e}.$$

We follow [10, 24] and define the numerical fluxes  $\hat{u}$  and  $\hat{\boldsymbol{\sigma}}$  for each  $T \in \mathcal{T}_h$  as follows:

$$\hat{u}_{T,e} := \begin{cases} \{u_h\} + \boldsymbol{\zeta} \cdot [u_h] & \text{if } e \subset \mathcal{E}_I \\ g & \text{if } e \subset \mathcal{E}_\partial \end{cases} \quad (7)$$

and

$$\hat{\boldsymbol{\sigma}}_{T,e} := \begin{cases} \{\boldsymbol{\sigma}_h\} - \boldsymbol{\zeta}[\boldsymbol{\sigma}_h] - \delta[u_h] & \text{if } e \subset \mathcal{E}_I \\ \boldsymbol{\sigma}_h - \delta(u_h - g) \mathbf{n} & \text{if } e \subset \mathcal{E}_\partial \end{cases} \quad (8)$$

where the auxiliary functions  $\delta$  (scalar) and  $\boldsymbol{\zeta}$  (vector) are univalued on each edge (face)  $e \in \mathcal{E}$  and must be chosen appropriately.

From the definitions (7) and (8), it follows that

$$\{\hat{u}\} = \hat{u}, \quad [\hat{u}] = 0, \quad \{\hat{\boldsymbol{\sigma}}\} = \hat{\boldsymbol{\sigma}}, \quad [\hat{\boldsymbol{\sigma}}] = 0, \quad \text{on } \mathcal{E}_I, \quad (9)$$

which implies that the numerical fluxes are consistent and conservative (see [1] or [10] for the corresponding definitions).

#### 4. The flux formulation

First of all, we recall from [9] that for  $v := (v_T)_{T \in \mathcal{T}_h} \in \Pi_{T \in \mathcal{T}_h} L^2(\partial T)$  and  $\boldsymbol{\tau} := (\boldsymbol{\tau}_T)_{T \in \mathcal{T}_h} \in \Pi_{T \in \mathcal{T}_h} [L^2(\partial T)]^d$ , we have the following identity:

$$\sum_{T \in \mathcal{T}_h} \int_{\partial T} v_T \boldsymbol{\tau} \cdot \mathbf{n}_T = \sum_{e \in \mathcal{E}_I} \int_e \{v\} [\boldsymbol{\tau}] + \sum_{e \in \mathcal{E}_I} \int_e [v] \cdot \{\boldsymbol{\tau}\} + \sum_{e \in \mathcal{E}_\partial} \int_e [v] \cdot \{\boldsymbol{\tau}\}. \quad (10)$$

Now, summing up in (6) over all the elements  $T \in \mathcal{T}_h$ , using the identity (10) and the properties (9), we have that

$$\left\{ \begin{array}{l} \int_{\Omega} \mathbf{s}_h \cdot \boldsymbol{\tau}_h + \int_{\Omega} u_h \nabla_h \cdot \boldsymbol{\tau}_h - \sum_{e \in \mathcal{E}_I} \int_e \hat{u}[\boldsymbol{\tau}_h] - \sum_{e \in \mathcal{E}_{\partial}} \int_e \hat{u} \boldsymbol{\tau}_h \cdot \mathbf{n} = 0, \\ \int_{\Omega} \sum_{i=1}^d \sum_{j=1}^d a_{ij}(u_h) (\mathbf{s}_h)_j (\mathbf{t}_h)_i - \int_{\Omega} \boldsymbol{\sigma}_h \cdot \mathbf{t}_h = 0, \\ \int_{\Omega} \sum_{i=1}^d \partial_{x_i, h} f_i(u_h) v_h + \int_{\Omega} \boldsymbol{\sigma}_h \cdot \nabla_h v_h - \sum_{e \in \mathcal{E}_I} \int_e \hat{\boldsymbol{\sigma}} \cdot [v_h] - \sum_{e \in \mathcal{E}_{\partial}} \int_e \hat{\boldsymbol{\sigma}} \cdot [v_h] = \int_{\Omega} l v_h, \end{array} \right. \quad (11)$$

where  $\nabla_h \cdot$  and  $\nabla_h$  denote, respectively, the piecewise-divergence and piecewise-gradient operators.

Integrating by parts the second term of the left-hand side of the first equation in (11), using the definition of the numerical flux  $\hat{u}$ , (7), and the identity (10), we deduce:

$$\int_{\Omega} \mathbf{s}_h \cdot \boldsymbol{\tau}_h - \int_{\Omega} \nabla_h u_h \cdot \boldsymbol{\tau}_h + \int_{\mathcal{E}_I} [u_h] \cdot (\{\boldsymbol{\tau}_h\} - \boldsymbol{\zeta}[\boldsymbol{\tau}_h]) + \int_{\mathcal{E}_{\partial}} u_h \boldsymbol{\tau}_h \cdot \mathbf{n} = \int_{\mathcal{E}_{\partial}} g \boldsymbol{\tau}_h \cdot \mathbf{n}, \quad (12)$$

where we denote  $\int_{\mathcal{E}_I} := \sum_{e \in \mathcal{E}_I} \int_e$  and  $\int_{\mathcal{E}_{\partial}} := \sum_{e \in \mathcal{E}_{\partial}} \int_e$ .

Similarly, using the definition of the flux  $\hat{\boldsymbol{\sigma}}$ , (8), the third equation of (11) is written as follows:

$$\begin{aligned} \int_{\Omega} \sum_{i=1}^d \partial_{x_i, h} f_i(u_h) v_h + \int_{\Omega} \boldsymbol{\sigma}_h \cdot \nabla_h v_h - \int_{\mathcal{E}_I} (\{\boldsymbol{\sigma}_h\} - \boldsymbol{\zeta}[\boldsymbol{\sigma}_h]) \cdot [v_h] + \int_{\mathcal{E}_I} \delta [u_h] \cdot [v_h] \\ - \int_{\mathcal{E}_{\partial}} \boldsymbol{\sigma}_h \cdot \mathbf{n} v_h + \int_{\mathcal{E}_{\partial}} \delta u_h v_h = \int_{\mathcal{E}_{\partial}} \delta g v_h + \int_{\Omega} l v_h. \end{aligned} \quad (13)$$

Summing up equation (13) to the second equation of (11) and taking into account (12) instead of the first equation of (11), we obtain

$$\left\{ \begin{array}{l} \int_{\Omega} \sum_{i=1}^d \partial_{x_i, h} f_i(u_h) v_h + \int_{\Omega} \sum_{i=1}^d \sum_{j=1}^d a_{ij}(u_h) (\mathbf{s}_h)_j (\mathbf{t}_h)_i - \int_{\Omega} \boldsymbol{\sigma}_h \cdot \mathbf{t}_h \\ + \int_{\Omega} \boldsymbol{\sigma}_h \cdot \nabla_h v_h - \int_{\mathcal{E}_I} (\{\boldsymbol{\sigma}_h\} - \boldsymbol{\zeta}[\boldsymbol{\sigma}_h]) \cdot [v_h] + \int_{\mathcal{E}_I} \delta [u_h] \cdot [v_h] - \int_{\mathcal{E}_{\partial}} \boldsymbol{\sigma}_h \cdot \mathbf{n} v_h \\ + \int_{\mathcal{E}_{\partial}} \delta u_h v_h = \int_{\mathcal{E}_{\partial}} \delta g v_h + \int_{\Omega} l v_h, \\ \int_{\Omega} \mathbf{s}_h \cdot \boldsymbol{\tau}_h - \int_{\Omega} \nabla_h u_h \cdot \boldsymbol{\tau}_h + \int_{\mathcal{E}_I} [u_h] \cdot (\{\boldsymbol{\tau}_h\} - \boldsymbol{\zeta}[\boldsymbol{\tau}_h]) + \int_{\mathcal{E}_{\partial}} u_h \boldsymbol{\tau}_h \cdot \mathbf{n} = \int_{\mathcal{E}_{\partial}} g \boldsymbol{\tau}_h \cdot \mathbf{n}. \end{array} \right. \quad (14)$$

Now, let us define the semilinear form  $A(\cdot, \cdot)$  by:

$$\begin{aligned} A((\mathbf{s}_h, u_h), (\mathbf{t}_h, v_h)) &:= \int_{\Omega} \sum_{i=1}^d \partial_{x_i, h} f_i(u_h) v_h + \int_{\Omega} \sum_{i=1}^d \sum_{j=1}^d a_{ij}(u_h) (\mathbf{s}_h)_j (\mathbf{t}_h)_i \\ &+ \int_{\mathcal{E}_I} \delta[u_h] \cdot [v_h] + \int_{\mathcal{E}_{\partial}} \delta u_h v_h, \end{aligned}$$

the bilinear form  $B(\cdot, \cdot)$  by:

$$B((\mathbf{t}_h, v_h), \boldsymbol{\sigma}_h) := - \int_{\Omega} \boldsymbol{\sigma}_h \cdot \mathbf{t}_h + \int_{\Omega} \boldsymbol{\sigma}_h \cdot \nabla_h v_h - \int_{\mathcal{E}_I} (\{\boldsymbol{\sigma}_h\} - \boldsymbol{\zeta}[\boldsymbol{\sigma}_h]) \cdot [v_h] - \int_{\mathcal{E}_{\partial}} \boldsymbol{\sigma}_h \cdot \mathbf{n} v_h,$$

and the functionals  $F$  and  $G$  by:

$$F(\mathbf{t}_h, v_h) := \int_{\mathcal{E}_{\partial}} \delta g v_h + \int_{\Omega} l v_h, \quad G(\boldsymbol{\tau}_h) := \int_{\mathcal{E}_{\partial}} g \boldsymbol{\tau}_h \cdot \mathbf{n},$$

for all  $(\mathbf{s}_h, u_h, \boldsymbol{\sigma}_h), (\mathbf{t}_h, v_h, \boldsymbol{\tau}_h) \in \Sigma_h^{k_1} \times V_h^{k_2} \times \Sigma_h^{k_3}$ . Then, problem (14) is equivalently written as follows:

$$\begin{cases} A((\mathbf{s}_h, u_h), (\mathbf{t}_h, v_h)) + B((\mathbf{t}_h, v_h), \boldsymbol{\sigma}_h) &= F(\mathbf{t}_h, v_h), \\ B((\mathbf{s}_h, u_h), \boldsymbol{\tau}_h) &= G(\boldsymbol{\tau}_h). \end{cases} \quad (15)$$

We remark that if  $\mathbf{f} = \mathbf{0}$ , that is, in the absence of convection, this formulation reduces to the one proposed in [9].

## 5. Numerical experiments

In this section, we consider  $d = 2$  and show some numerical results for the steady-state compressible Reynolds lubrication equation modified for slip flow.

We solve problem (3) with Dirichlet boundary conditions using the method described in the previous sections. To this end, we first rewrite the problem following the notations of Section 3. We define

$$f_1(u) = H u, \quad f_2(u) = 0, \quad A(u) = (\alpha + \beta H u) H^2 I$$

where  $u$  now denotes the pressure  $P$  and  $I \in \mathcal{M}_{2 \times 2}$  is the identity matrix.

We consider four tests. The first one consists of a problem with a known solution and is used to study the convergence properties of different schemes. After this study, we consider three tests where we solve the modified compressible Reynolds equation for slip flow with different air gap thicknesses.

Let us consider the function  $\mathbf{h}$  in  $L^\infty(\mathcal{E})$  related to the local meshsize as follows:

$$\mathbf{h} := \begin{cases} \min(h_T, h_{T'}) & \text{if } x \in \text{int}(\partial T \cap \partial T'), \\ h_T & \text{if } x \in \text{int}(\partial T \cap \Gamma), \end{cases}$$

where  $h_T$  denotes the diameter of an element  $T \in \mathcal{T}_h$ . Then, in all numerical experiments we chose

$$\delta = \frac{1}{\mathbf{h}} \quad \text{and} \quad \boldsymbol{\zeta} = \begin{pmatrix} 1 \\ 1 \end{pmatrix}.$$

Along this section, we denote by  $\|\cdot\|$  the  $L^2(\Omega)$  or  $[L^2(\Omega)]^2$ -norm. Moreover, we consider the usual energy norm  $\|\cdot\|_h$ , given by

$$\|v\|_h = \left( \|\nabla_h v\|^2 + \|\delta^{1/2}[v]\|_{[L^2(\mathcal{E}_I)]^2}^2 + \|\delta^{1/2}v\|_{L^2(\mathcal{E}_\partial)}^2 \right)^{1/2}$$

which is well defined for functions in the space  $V_h^k + H^1(\Omega)$ .

Since problem (3) is the adimensional form of (1), adimensional  $(X_1, X_2)$  variables are used in the presentation of the computational problems, while real  $(x_1, x_2)$  variables are used in the graphical representation of results.

For the implementation of the algorithms, we have used the FEniCS finite element package [21]. In some cases, we have improved the numerical algorithm with a simple *a priori* refinement strategy. More precisely, we have just refined the triangles in which the solution or its gradient is expected to be large.

*Test 1: Numerical convergence study*

We let  $\Omega = (0, 1) \times (0, 1)$ , the thickness  $H(X_1, X_2) = 2 - X_1$ ,  $\alpha = 0.003$ ,  $\beta = 0.0007$  and the exact solution

$$u(X_1, X_2) = 1.0 + \sin(0.5 \pi X_1) \cos(0.5 \pi X_2), \quad (X_1, X_2) \in \Omega.$$

Given two consecutive meshes of mesh sizes  $h_1$  and  $h_2$ , the rate of convergence for a given variable  $\xi$ ,  $r(\xi)$ , is computed as

$$r(\xi) = \frac{\ln \frac{\|\xi - \xi_{h_1}\|}{\|\xi - \xi_{h_2}\|}}{\ln\left(\frac{h_1}{h_2}\right)},$$

where  $\xi_{h_i}$  is the approximation of  $\xi$  obtained with the mesh of size  $h_i$  ( $i = 1, 2$ ). Analogously, we define the rate of convergence for variable  $u$  in the energy norm as:

$$r_h(u) = \frac{\ln \frac{\|u - u_{h_1}\|_h}{\|u - u_{h_2}\|_h}}{\ln\left(\frac{h_1}{h_2}\right)}.$$

The total error,  $e_{\text{total}}$ , is computed as follows:

$$e_{\text{total}} := \left( \|u - u_h\|_h^2 + \|\mathbf{s} - \mathbf{s}_h\|^2 + \|\boldsymbol{\sigma} - \boldsymbol{\sigma}_h\|^2 \right)^{1/2}.$$

In Tables 1-5 we show the errors for the unknowns  $u$ ,  $\mathbf{s}$  and  $\boldsymbol{\sigma}$  in the corresponding norms, and the associated rates of convergence as well as the global rate of convergence  $r$  for the different meshes and degrees of approximation. We use polynomials of degree  $k = 1, 2, 3$  for the pressure  $u$  and  $l = k - 1$  or  $k$  to approximate the pressure gradient  $\mathbf{s}$  and the total flux  $\boldsymbol{\sigma}$ .

We use uniform meshes of triangles with  $n = 1/h$  elements on each side of  $\Omega$ . The nonlinear system of equations is solved using a Newton-Krylov method. The algorithms do 3 or 4 Newton iterations with a mixed stopping criterion on both the absolute tolerance and the relative tolerance of  $10^{-10}$ .

In Tables 1 and 2 we can observe that the global rate of convergence of the algorithm is around one.

For  $k = 2$  and  $l = 1$ , we observe quadratic convergence in the pressure both in the  $L^2$ -norm and in the energy norm. However, the method stagnates in the remaining variables (see Table 3). In Table 4 ( $k = l = 2$ ) we observe convergence of order 2 in all variables.

Finally, in Table 5 we see that the method converges with order 3 in all variables for  $k = 3$  and  $l = 2$ .

*Test 2: Compressible Reynolds lubrication equation*

We let  $\Omega = (0, 1) \times (0, 1)$ ,  $\alpha = \beta = 0.003$  and  $P = 1$  on  $\Gamma$ . We follow [6, p. 757] and solve the compressible Reynolds lubrication equation with

$$H(X_1, X_2) = 2 - X_1, \quad (X_1, X_2) \in \Omega.$$

Figure 1 shows the final mesh and the  $\mathcal{P}_1$ -approximation of the pressure. We have performed six refinement steps, which provide a better approximation of the solution in the region where a boundary layer is present. The numerical solution is in accordance with the results obtained in [4].

*Test 3: Compressible Reynolds lubrication equation with a cylindrical head*

We let  $\Omega = (0, 1) \times (0, 1)$ ,  $\alpha = 0.1$  and  $\beta = 0.03$  and  $P = 1$  on  $\Gamma$ . We solve the compressible Reynolds lubrication equation with a cylindrical head, which gives rise to the following gap function:

$$H(X_1, X_2) := 1 + (X_1 - 0.5)^2, \quad (X_1, X_2) \in \Omega.$$

In Figure 2 we show the grid and the  $\mathcal{P}_1$ -approximation of the pressure obtained with the algorithm. In this case the grid has been refined near the line  $X_1 = \frac{1}{2}$ , where the highest pressure is expected, and near  $X_1 = 1$ , where a drop of pressure is appreciated due to the fact that the gap becomes larger.

*Test 4: Compressible Reynolds lubrication equation in the presence of discontinuous gaps*

With the aim of improving the read/write process, designers and manufacturers introduce one or several slots in the reading head. Thus, the gap function becomes discontinuous.

Let us consider the same domain,  $\Omega$ , parameters  $\alpha$  and  $\beta$  and boundary condition of the previous test, and a gap function given by:

$$H(X_1, X_2) := \begin{cases} 1.2 & \text{if } (X_1, X_2) \in (0.2, 0.4) \times (0.475, 0.525) \\ 1.2 & \text{if } (X_1, X_2) \in (0.6, 0.8) \times (0.475, 0.525) \\ 1 + (X_1 - 0.5)^2 & \text{otherwise.} \end{cases}$$

Figure 3 shows the computational mesh and the  $\mathcal{P}_1$ -approximation of the pressure obtained with the implemented algorithm. The mesh presents an a priori refinement around the slots. We can appreciate the effect of the slots, mainly in the drop of pressure around the line  $X_2 = 0.5$ .

The numerical pressure is qualitatively different to the one presented in [4]. There, a characteristics method combined with duality methods were applied. A discontinuous Galerkin method like the one described in the present work seems more adequate to this kind of problems due to the discontinuities of the gap function  $H$ .

Let us remark that the numerical approximation of the pressure is very similar when using a more realistic value of the coefficient of the nonlinear diffusion term, as  $\beta = 7 \times 10^{-4}$ . Just a slight drop of the pressure is appreciated in the mid region of the device, over the slots.

## 6. Conclusions

We proposed a new discontinuous Galerkin method to solve stationary nonlinear convection-diffusion problems based on the introduction of the gradient  $\mathbf{s}$  and the total flux  $\boldsymbol{\sigma}$  as additional unknowns. This method can be viewed as an extension of the method proposed in [9] for nonlinear diffusion problems.

We applied the new method to the numerical solution of the compressible Reynolds lubrication equation modified for slip flow. We developed a numerical convergence study where we found that the method converges with order 1 when all unknowns are approximated by piecewise linear polynomials and also when the pressure is approximated by a piecewise linear polynomial and the gradient and the total flux are approximated by piecewise constants. The method converges with order 2 when all unknowns are approximated by piecewise quadratic polynomials. However, it stagnates in the gradient and the total flux when the pressure is approximated by piecewise quadratic polynomials and  $\mathbf{s}$  and  $\boldsymbol{\sigma}$  are approximated by piecewise linear polynomials. Finally, the method converges with order 3 when the pressure is approximated by piecewise cubic polynomials and piecewise quadratic polynomials are used to approximate the gradient and the total flux.

We also solved the equation under different configurations; in particular, one of the experiments include a realistic discontinuous gap function. This kind of problems are the practical reason for introducing discontinuous Galerkin methods.

## Acknowledgements

This research was partially supported by the Spanish Ministerio de Economía y Competitividad under grants MTM2013-47800-C2-1-P and MTM2016-76497-R.

## References

- [1] D.N. Arnold, F. Brezzi, B. Cockburn and L.D. Marini, Unified analysis of discontinuous Galerkin methods for elliptic problems, *SIAM J. Numer. Anal.* 39 (2002) 1749-1779.
- [2] I. Arregui, J.J. Cendán and C. Vázquez, A duality method for the compressible Reynolds equation. Application to simulation of read/write processes in magnetic storage devices, *J. Comput. Appl. Math.* 175 (2005) 1, 31-40.
- [3] I. Arregui, J.J. Cendán and C. Vázquez, Numerical simulation of head/tape magnetic reading devices by a new 2-D model, *Finite Elements in Analysis and Design* 43 (2007) 4, 311-320.
- [4] I. Arregui, J.J. Cendán and C. Vázquez, Adaptive numerical methods for an hydrodynamic problem arising in magnetic reading devices, *Math. Comput. Simulation* 99 (2014) 190-202.
- [5] F. Bassi and S. Rebay, A high-order accurate discontinuous finite element method for the numerical solution of the compressible Navier-Stokes equations, *J. Comput. Phys.* 131 (1997) 267-279.
- [6] B. Bhushan, *Tribology and Mechanics of Magnetic Storage Devices*, Springer, New York, 1990.
- [7] A. Buffa, T.J.R. Hughes and G. Sangalli, Analysis of a multiscale discontinuous Galerkin method for convection-diffusion problems, *SIAM J. Numer. Anal.* 44 (2006) 4, 1420-1440.
- [8] A. Burgdorfer, The influence of the molecular mean-free path on the performance of hydrodynamic gas lubricated bearings, *Trans. ASME, Part D (J. Basic Engineering)* 81 (1959) 94-100.
- [9] R. Bustinza and G.N. Gatica, A local discontinuous Galerkin method for nonlinear diffusion problems with mixed boundary conditions, *SIAM J. Sci. Comp.* 26 (2004) 1, 152-177.
- [10] P. Castillo, B. Cockburn, I. Perugia and D. Schötzau, An a priori error analysis of the local discontinuous Galerkin method for elliptic problems, *SIAM J. Numer. Anal.* 38 (2000) 5, 1676-1706.
- [11] J.J. Cendán Verdes, *Estudio matemático y numérico del modelo de Reynolds-Koiter y de los modelos tribológicos en lectura magnética*, Ph. D. Dissertation, Publicacións do Departamento de Matemática Aplicada II, Universidade de Vigo, 2005.
- [12] M. Chipot and M. Luskin, Existence and uniqueness of solutions to the compressible Reynolds lubrication equation, *SIAM J. Math. Anal.* 17 (1986) 6, 1390-1399.

- [13] M. Chipot and M. Luskin, The compressible Reynolds lubrication equation, Metastability and incompletely posed problems, 61-75, IMA Vol. Math. Appl., 3, Springer, New York, 1987.
- [14] E.T. Chung and W.T. Leung, A sub-grid structure enhanced discontinuous Galerkin method for multiscale diffusion and convection-diffusion problems, Commun. Comput. Phys. 14 (2013) 2, 370-392.
- [15] B. Cockburn, B. Dong, J. Guzmán, M. Restelli and R. Sacco, A hybridizable discontinuous Galerkin method for steady-state convection-diffusion-reaction problems, SIAM J. Sci. Comput. 31 (2009) 5, 3827-3846.
- [16] B. Cockburn and C.-W. Shu, The local discontinuous Galerkin method for time-dependent convection-diffusion systems, SIAM J. Numer. Anal. 35 (1998) 2440-2463.
- [17] H. Egger and J. Schöberl, A hybrid mixed discontinuous Galerkin finite-element method for convection-diffusion problems, IMA J. Numer. Anal. 30 (2010) 1206-1234.
- [18] T.J.R. Hughes, G. Scovazzi, P. Bochev and A. Buffa, A multiscale discontinuous Galerkin method with the computational structure of a continuous Galerkin method, Comput. Meth. Appl. Mech. Engrg. 195 (2006) 2761-2787.
- [19] M. Jai, Homogenization and two-scale convergence of the compressible Reynolds lubrication equation modelling the flying characteristics of a rough magnetic head over a rough rigid-disk surface. RAIRO Modél. Math. Anal. Numér. 29 (1995) 2, 199-233.
- [20] M.-Y. Kim and M.F. Wheeler, A multiscale discontinuous Galerkin method for convection-diffusion-reaction problems, Comp. Maths. Appl. 68 (2014) 2251-2261.
- [21] A. Logg, K.-A. Mardal and G. Wells (Eds.), Automated Solution of Differential Equations by the Finite Element Method. The FEniCS Book, Springer, 2012.
- [22] N.C. Nguyen, J. Peraire and B. Cockburn, An implicit high-order hybridizable discontinuous Galerkin method for linear convection-diffusion equations, J. Comput. Physics 228 (2009) 3232-3254.
- [23] N.C. Nguyen, J. Peraire and B. Cockburn, An implicit high-order hybridizable discontinuous Galerkin method for nonlinear convection-diffusion equations, J. Comput. Physics 228 (2009) 8841-8855.
- [24] I. Perugia and D. Schötzau, An hp-analysis of the local discontinuous Galerkin method for diffusion problems, J. Sci. Comp. 17 (2002) 561-571.

- [25] W. Reed and T. Hill, Triangular mesh methods for the neutron transport equation. Tech. Report LA-UR-73-479, 1973.
- [26] Y. Wu and F. E. Talke, A finite element simulation of the two-dimensional head/tape interface for head contours with longitudinal bleed slots, Tribol. Int. 33 (2000) 123-130.
- [27] Y. Yang and P. Zhu, Discontinuous Galerkin methods with interior penalties on graded meshes for 2D singularly perturbed convection-diffusion problems, Appl. Numer. Math. 111 (2017) 36-48.

$h$	$\ u - u_h\ $	$r(u)$	$\ u - u_h\ _h$	$r_h(u)$	$\ \mathbf{s} - \mathbf{s}_h\ $	$r(\mathbf{s})$	$\ \boldsymbol{\sigma} - \boldsymbol{\sigma}_h\ $	$r(\boldsymbol{\sigma})$	$e_{\text{total}}$	$r$
$\frac{1}{5}$	1.45E-02	-	1.97E-01	-	1.58E-01	-	1.58E-03	-	2.52E-01	-
$\frac{1}{10}$	5.20E-03	1.49	1.03E-01	0.94	8.77E-02	0.85	8.06E-04	0.97	1.35E-01	0.90
$\frac{1}{20}$	1.94E-03	1.42	4.95E-02	1.05	4.43E-02	0.99	3.91E-04	1.04	6.64E-02	1.02
$\frac{1}{40}$	8.44E-04	1.20	2.40E-02	1.04	2.20E-02	1.01	1.94E-04	1.01	3.26E-02	1.03
$\frac{1}{80}$	3.93E-04	1.10	1.17E-02	1.03	1.08E-02	1.02	9.69E-05	1.00	1.60E-02	1.03
$\frac{1}{160}$	1.89E-04	1.05	5.79E-03	1.02	5.37E-03	1.02	4.84E-05	1.00	7.89E-03	1.02

Table 1: Test 1: Errors and rates of convergence for  $k = 1$  and  $l = 0$

$\bar{h}$	$\ u - u_h\ $	$r(u)$	$\ u - u_h\ _h$	$r_h(u)$	$\ \mathbf{s} - \mathbf{s}_h\ $	$r(\mathbf{s})$	$\ \boldsymbol{\sigma} - \boldsymbol{\sigma}_h\ $	$r(\boldsymbol{\sigma})$	$e_{\text{total}}$	$r$
$\frac{1}{5}$	1.12E-02	-	2.22E-01	-	1.82E-02	-	1.92E-03	-	2.84E-01	-
$\frac{1}{10}$	3.73E-03	1.59	1.10E-01	0.99	9.36E-02	0.96	9.64E-04	0.99	1.44E-01	0.98
$\frac{1}{20}$	1.33E-03	1.49	5.35E-02	1.04	4.68E-02	1.00	4.38E-04	1.00	7.11E-02	1.02
$\frac{1}{40}$	5.64E-04	1.24	2.63E-02	1.02	2.34E-02	1.00	2.43E-04	0.99	3.52E-02	1.01
$\frac{1}{80}$	3.73E-04	1.12	1.30E-02	1.02	1.17E-02	1.00	1.22E-04	0.99	1.75E-02	1.01

Table 2: Test 1: Errors and rates of convergence for  $k = 1$  and  $l = 1$

$h$	$\ u - u_h\ $	$r(u)$	$\ u - u_h\ _h$	$r_h(u)$	$\ \mathbf{s} - \mathbf{s}_h\ $	$r(\mathbf{s})$	$\ \boldsymbol{\sigma} - \boldsymbol{\sigma}_h\ $	$r(\boldsymbol{\sigma})$	$e_{\text{total}}$	$r$
$\frac{1}{5}$	4.07E-04	-	2.02E-02	-	1.15E+00	-	1.31E-02	-	1.15E+00	-
$\frac{1}{10}$	7.67E-05	2.41	5.06E-03	2.00	1.18E+00	0.04	1.34E-02	0.03	1.18E+00	-0.04
$\frac{1}{20}$	1.27E-05	2.59	1.20E-03	2.07	1.19E+00	0.01	1.35E-02	0.01	1.19E+00	-0.01
$\frac{1}{40}$	2.39E-06	2.41	2.89E-04	2.05	1.20E+00	0.01	1.36E-02	0.01	1.20E+00	-0.01
$\frac{1}{80}$	5.02E-07	2.25	7.13E-05	2.02	1.20E+00	0.00	1.36E-02	0.00	1.20E+00	-0.00

Table 3: Test 1: Errors and rates of convergence for  $k = 2$  and  $l = 1$

$h$	$\ u - u_h\ $	$r(u)$	$\ u - u_h\ _h$	$r_h(u)$	$\ \mathbf{s} - \mathbf{s}_h\ $	$r(\mathbf{s})$	$\ \boldsymbol{\sigma} - \boldsymbol{\sigma}_h\ $	$r(\boldsymbol{\sigma})$	$e_{\text{total}}$	$r$
$\frac{1}{5}$	3.33E-04	-	1.07E-02	-	8.93E-03	-	9.27E-05	-	1.39E-02	-
$\frac{1}{10}$	6.23E-05	2.44	2.77E-03	1.95	2.31E-03	1.95	2.42E-05	1.94	3.60E-03	1.95
$\frac{1}{20}$	1.18E-05	2.41	6.34E-04	2.12	5.46E-04	2.08	5.61E-06	2.11	8.37E-04	2.11
$\frac{1}{40}$	2.54E-06	2.21	1.44E-04	2.14	1.28E-04	2.09	1.32E-06	2.08	1.93E-04	2.12

Table 4: Test 1: Errors and rates of convergence for  $k = 2$  and  $l = 2$

$h$	$\ u - u_h\ $	$r(u)$	$\ u - u_h\ _h$	$r_h(u)$	$\ \mathbf{s} - \mathbf{s}_h\ $	$r(\mathbf{s})$	$\ \boldsymbol{\sigma} - \boldsymbol{\sigma}_h\ $	$r(\boldsymbol{\sigma})$	$e_{\text{total}}$	$r$
$\frac{1}{5}$	2.79E-05	-	1.02E-03	-	8.29E-04	-	8.21E-06	-	1.31E-03	-
$\frac{1}{10}$	2.89E-06	3.27	1.19E-04	3.10	1.03E-04	3.02	9.96E-07	3.04	1.57E-04	3.07
$\frac{1}{20}$	3.31E-07	3.12	1.42E-05	3.06	1.26E-05	3.03	1.22E-07	3.03	1.90E-05	3.05
$\frac{1}{40}$	3.86E-08	3.10	1.69E-06	3.07	1.53E-06	3.04	1.50E-08	3.03	2.28E-06	3.05

Table 5: Test 1: Errors and rates of convergence for  $k = 3$  and  $l = 2$

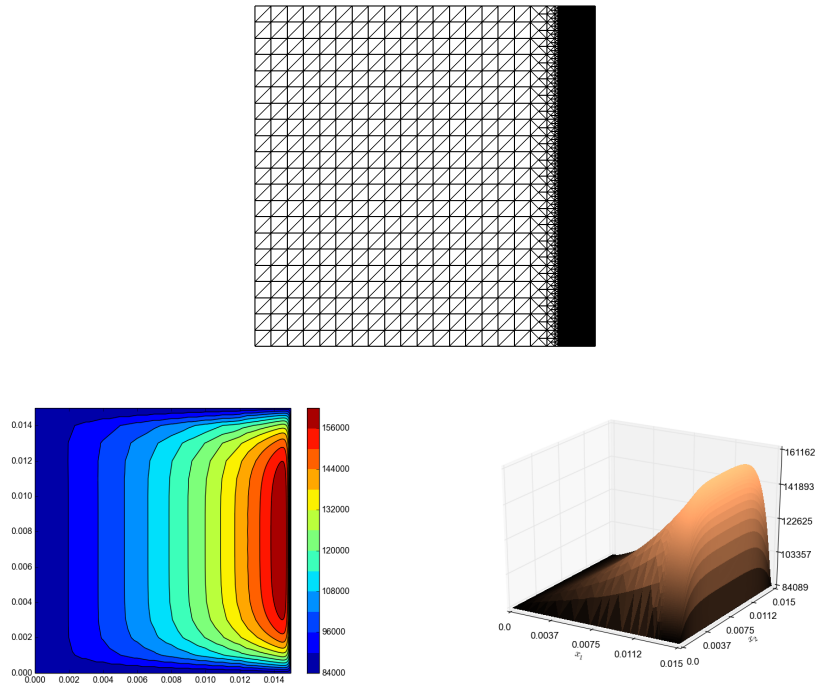


Figure 1: Test 2: Mesh with 337 302 dof and  $\mathcal{P}_1$  approximation of the pressure for  $k = 1$  and  $l = 0$

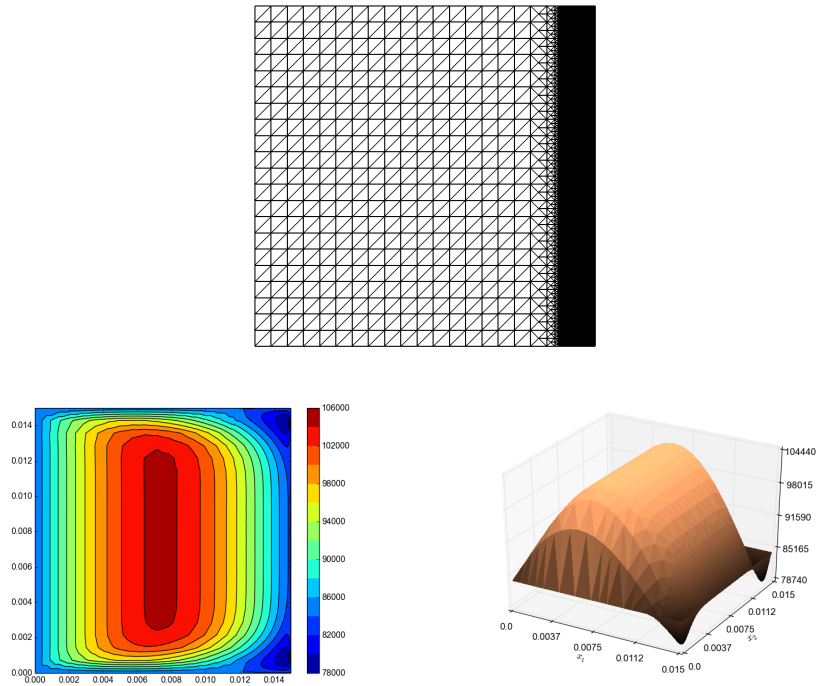


Figure 2: Test 3: Mesh with 648 711 dof and  $\mathcal{P}_1$  approximation of the pressure for  $k = 1$  and  $l = 0$

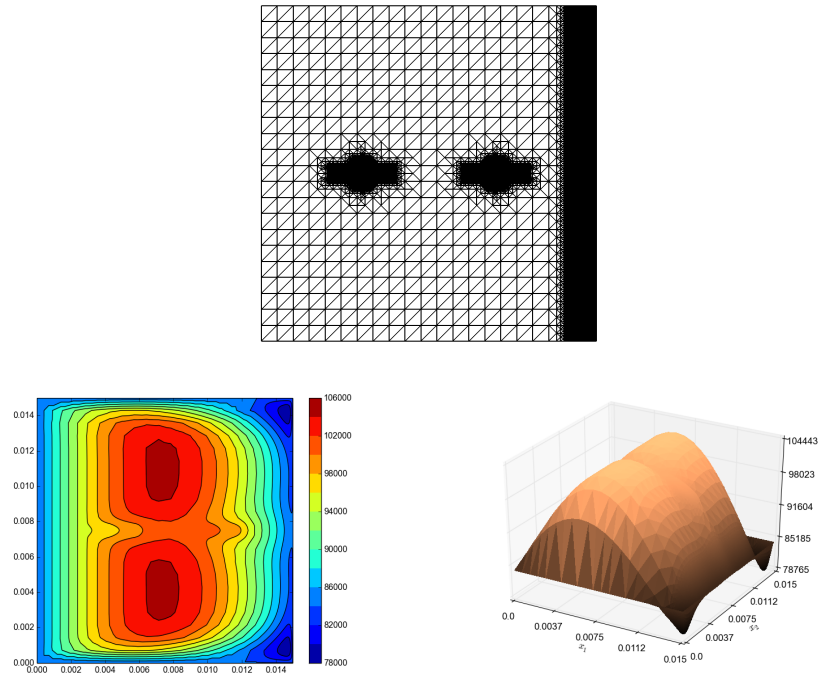


Figure 3: Test 4: Mesh with 756 399 dof and  $\mathcal{P}_1$  approximation of the pressure for  $k = 1$  and  $l = 0$